

# Estimate of recharge from radiocarbon dating of groundwater and numerical flow and transport modeling

Chen Zhu

Department of Geology and Planetary Science, University of Pittsburgh, Pittsburgh, Pennsylvania

**Abstract.** This paper combines radiocarbon age and hydraulic data to estimate recharge to a regional groundwater aquifer. The  $^{14}\text{C}$  ages of groundwater are first corrected for the effects of chemical reactions through geochemical modeling. Recharge rates to the aquifer are then calibrated to observed  $^{14}\text{C}$  ages using a linked numerical  $^{14}\text{C}$  transport and flow model while hydraulic conductivity values are proportionally adjusted to match observed heads. The methodology is general but has particular applications to semiarid and arid regions where the need for reliable recharge estimates is greatest but the task is the most difficult. The ability of this method for estimating recharge on the scale of thousands of years makes it a valuable tool for studies of global environmental changes and performance assessment of radioactive waste repositories. A case study of a regional aquifer in northeastern Arizona shows the recharge estimates are within the bounds determined by chloride mass balance but are significantly higher than previous estimates derived from the Maxey-Eakin method.

## 1. Introduction

Although both the physical processes that control groundwater flow in saturated porous media and their mathematical representations are well understood [*National Research Council (NRC), 1990*], the accuracy and usefulness of groundwater flow models is challenged by the difficulties of obtaining site-specific hydraulic parameters and boundary conditions necessary for approximating groundwater flow. Among the hydraulic parameters, recharge rates are one of the most poorly constrained in almost all groundwater flow and transport models [*Lerner et al., 1990; Anderson and Woessner, 1992*]. However, recharge is an important component of the water budget, especially in models evaluating water resource sustainability. The problem of lacking reliable recharge estimates becomes more prominent for model applications in arid and semiarid environments, where the recharge flux is low and highly variable [*Lerner et al., 1990*].

Various field methods of recharge estimates in semiarid and arid regions have been recently reviewed by *Gee and Hillel [1988]*, *Allison [1988]*, *Lerner et al. [1990]*, *Allison et al. [1994]*, *Phillips [1994]*, and *Hendrickx and Walker [1997]*. They concluded that because of the temporal and spatial variability of the measured properties and the issue of preferential flow, field measurements generally carry large uncertainties and are difficult to extrapolate to regional scale. Therefore, in practice, recharge is often used as an adjustable parameter during model calibration [*Anderson and Woessner, 1992*]. However, because hydraulic conductivity can vary over 13 orders of magnitude [*Freeze and Cherry, 1979*], a practically infinite number of combinations of hydraulic conductivities and recharge rates that span a wide range could all match the target head distribution for a flow model calibration. Consequently, inadequate controls of recharge rates can lead to an acute situation of nonuniqueness of flow model solutions, which may render

many water resource management models unusable [*Brooks et al., 1994*].

It appears that for recharge rates to be used in simulating groundwater flow in regional scale aquifers, better estimates may be found from environmental isotopic tracers in the saturated zone, where the numerous problems associated with the unsaturated zone can be circumvented. In this paper, we use  $^{14}\text{C}$  dating of groundwater from the saturated zone and a linked numerical flow and transport model to estimate recharge fluxes. We contend that groundwater recharge calculated from this method is better suited for use in regional-scale flow and transport models. This method first calls for correction of  $^{14}\text{C}$  groundwater ages through geochemical modeling of water-rock interactions. The age data together with hydraulic heads become the targets for simultaneous calibration of recharge rates and hydraulic conductivity, through comparing observed ages and heads with those simulated by the linked flow/ $^{14}\text{C}$  transport model.

The potential of  $^{14}\text{C}$  data to calibrate flow parameters has long been recognized, and the methodology outlined above has been applied to estimate recharge rates [e.g., *Campana and Simpson, 1984; Adar and Neuman, 1988*]. However, earlier applications used mixing cell or discrete-state compartment models, which are limited by their approximation in treating flow and mixing. *Phillips et al. [1989]* pointed out that the use of a distributed parameter model is the “elegant” approach because aquifer geometry and hydraulic head fields as well as dispersive-diffusive parameters and hydraulic conductivities are specified, and the system is studied as a whole. This approach has been applied in recent years using groundwater ages (younger than a few decades) estimated from nonreactive tracers (CFCs,  $^3\text{H}$ , and  $^3\text{H}/^3\text{He}$ ) to constrain recharge, dispersivity, and hydraulic conductivity for shallow, small-scale, unconfined aquifers [*Robertson and Cherry, 1989; Solomon and Sudicky, 1991; Reilly et al., 1994; Portniaguine and Solomon, 1998*]. It is shown in this study that the flow/transport model approach can also be applied to the reactive tracer radiocarbon ( $^{14}\text{C}$ ), when a two-step approach is taken to separate the geo-

Copyright 2000 by the American Geophysical Union.

Paper number 2000WR900172.  
0043-1397/00/2000WR900172\$09.00

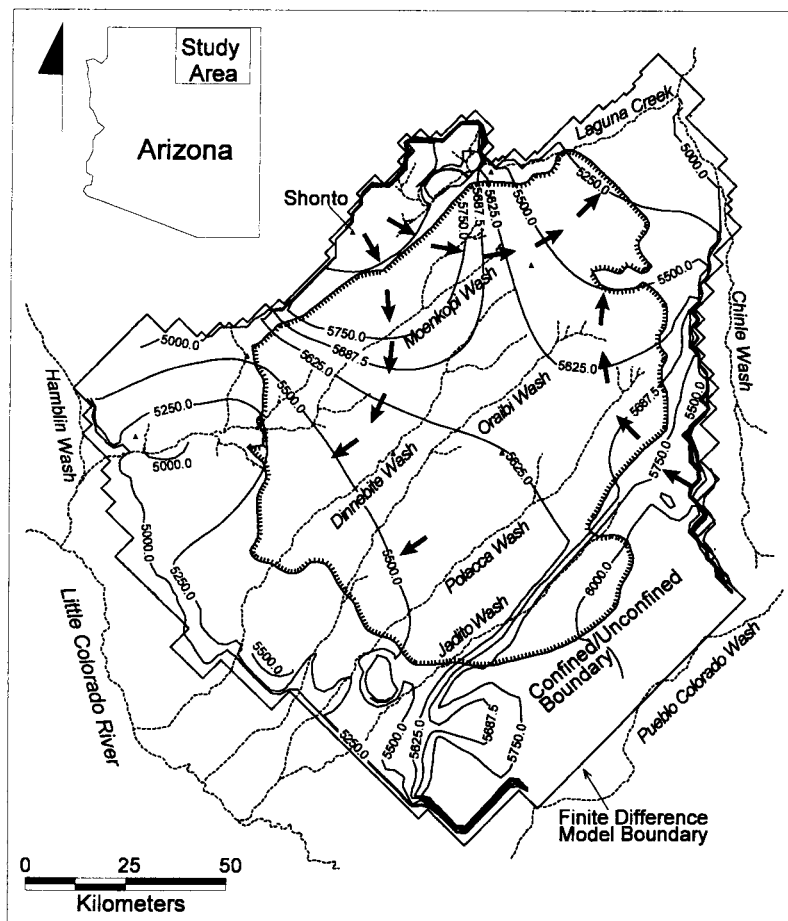


**Figure 1.** Simulated contours of present-day hydraulic heads (in feet (1 foot = 0.3048 m)) generated from the calibrated two-dimensional finite difference flow model developed by GeoTrans (personal communication, 1987). Arrows indicate the directions of groundwater flow. Also shown are the finite difference model and the confined/unconfined aquifer boundaries.

chemical reactions and physical transport processes. Radiocarbon's half-life and ubiquitous occurrence makes this methodology broadly useful in studying regional-scale aquifers.

In this study, the method is applied to a regional aquifer in semiarid-arid northeastern Arizona (Figure 1). This application allows examining the details of this method and demonstrating its applicability. The application to this heavily studied area illustrates the inadequacy of models that rely on hydraulic data alone and the potential of using geochemical and isotopic data to better constrain the rate and directions of groundwater flow.

## 2. Geologic and Hydrological Settings of the Study Area

The N aquifer in the Black Mesa basin, Arizona, is a 14,000 km<sup>2</sup> regional aquifer and an important source of potable water for the region (Figures 1 and 2). Studies of its stratigraphy and lithology, hydrogeology, and geochemistry have been well documented [Repenning and Page, 1956; Harshbarger et al., 1957; Kister and Hatchett, 1963; Cooley et al., 1969; Levings and Farrar, 1977a, 1977b, 1977c, 1977d; Farrar, 1979, 1980; Eychaner, 1983; Brown and Eychaner, 1988; Dulaney, 1989; Wickham, 1992; Griffith, 1993]. The Black Mesa Monitoring Program

performed by the U.S. Geological Survey (USGS) since 1971 has collected a large amount of water level and water quality data in the area [Hill, 1985; Hill and Sottolare, 1987; Hill and Whetten, 1986; Hart and Sottolare, 1988, 1989; Littin, 1992, 1993; Littin and Monroe, 1995]. The extensive hydrological data for Black Mesa have been organized and synthesized in three previous numerical modeling efforts. Eychaner [1983] and Brown and Eychaner [1988] developed two-dimensional, finite difference regional groundwater flow models; the latter used the USGS program MODFLOW [McDonald and Harbaugh, 1988]. GeoTrans (unpublished report, 1987) developed a similar two-dimensional regional groundwater flow model for Black Mesa. All three flow models were primarily based on hydraulic data alone. In a more recent study, Zhu et al. [1998] found that the paleohydrogeology in the N aquifer was significantly influenced by paleoclimate changes during late Pleistocene and Holocene.

Black Mesa is a prominent topographic high ~150–300 m above the surrounding area and occupies the structural center of the Black Mesa basin. Sedimentary rocks from Permian to late Tertiary, which range in thickness from 300 to 3000 m, overlie the Precambrian to Cambrian granitic and metamorphic basement rocks. Regional movements of groundwater are restricted to the C, D, and N multiple aquifer systems [Cooley

*et al.*, 1969]. In general, water table conditions prevail at the flanks of the basin, while artesian conditions prevail in the center of the mesa.

The Upper Triassic/Lower Jurassic N aquifer consists of four formations: the Wingate Sandstone, Moenave Formation, Kayenta Formation, and Navajo Sandstone. The N aquifer overlies the Chinle Formation and is overlain unconformably by the Carmel Formation (Figure 3). Productive water-bearing units in the N aquifer are predominantly the Navajo Sandstone, followed by the Lukachukai member of the Wingate Sandstone.

The Navajo Sandstone in the Black Mesa area has relatively uniform lithology and is of aeolian origin [Harshbarger *et al.*, 1957]. The sandstone is composed of medium- to fine-grained quartz sands [Harshbarger *et al.*, 1957; Dulaney, 1989]. Other types of sand grains include mostly plagioclase and, to a lesser extent, orthoclase [Harshbarger *et al.*, 1957; Dulaney, 1989]. The feldspar content is typically 2% [Harshbarger *et al.*, 1957]. Small amounts of biotite and muscovite also occur in the Navajo Sandstone. The sandstone is cemented by calcite and, to a lesser extent, by silica, and red iron oxide rims are common on the sand grains [Harshbarger *et al.*, 1957; Dulaney, 1989]. Clay minerals appear as alteration products of plagioclase [Dulaney, 1989]. The clay minerals identified by X-ray diffraction and microscopy include smectite, illite, kaolinite, and glauconite.

Groundwater in the N aquifer moves southeast from the Shonto area toward the center of the mesa, where the flow path diverges northeastward toward Laguna Creek and Chinle Wash and southwestward toward Moenkopi Wash [Cooley *et al.*, 1969; Brown and Eychaner, 1988] (Figure 1). The aquifer is

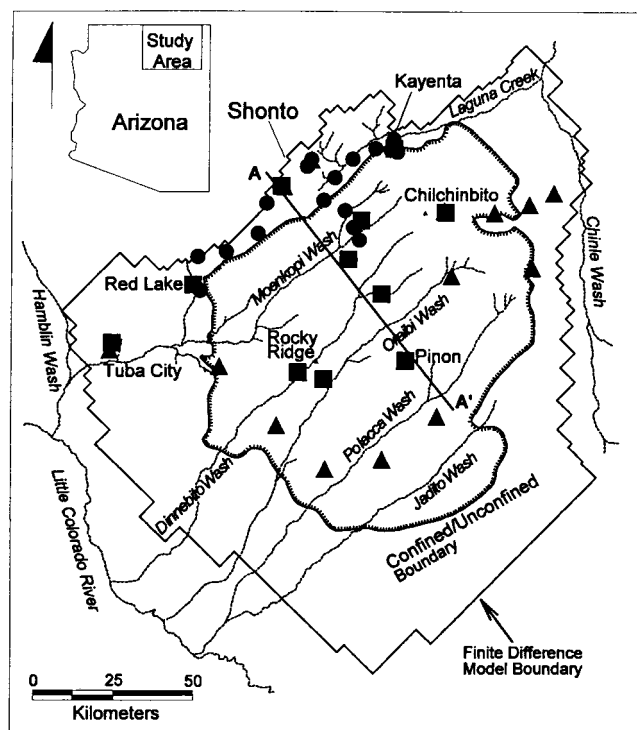


**Figure 2.** Location of groundwater samples for radiocarbon analysis and surface water features. Solid circles, this study; triangles, Wickham [1992]; squares, Lopes and Hoffman [1997]. The line A-A' indicates the approximate location of the cross section in Figure 3.

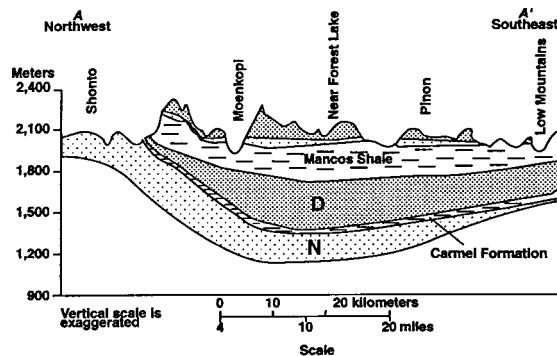


**Figure 3.** Cross section of the Black Mesa basin. The location is indicated in Figure 2. N and D stand for the N and D aquifer. The shaly Carmel Formation hydraulically separates the N and D aquifers. The D aquifer is overlain by the Mancos Shale. Modified from Cooley *et al.* [1969].

recharged seasonally from the precipitation in the highlands principally during the winter and spring. The Shonto area accounts for approximately one third of the total recharge in the basin and most water that flows into the center of the basin [Cooley *et al.*, 1969]. The principal discharge areas are along the Moenkopi Wash near Tuba City and into the alluvium along Dinnebito and Oraibi Washes.

The D aquifer overlies the N aquifer throughout the Black Mesa area (Figure 3), but the D is less productive than the N. The D aquifer is overlain by the 130–200 m thick, confining Mancos Shale which hydraulically separates the D from overlying formations. Groundwater in the D aquifer moves from the east and northeast to the west and southwest [Wickham, 1992]. Discharge is to the flood plain alluvium along the tributaries to the Little Colorado River and, to a lesser degree in the north, along the tributaries to Chinle Wash [Cooley *et al.*, 1969]. Large differences in hydraulic head between the D and N aquifers are reported [Wickham, 1992], with the largest difference being as much as 200 m. Groundwater from the D aquifer is characterized by high total dissolved solids (TDS) (see Table 1 for a list of notations and symbols), elevated  $\text{SO}_4^{2-}$ ,  $\text{Cl}^-$ , and  $\text{Na}^+$  concentrations, and lower dissolved oxygen (DO). Leaking of D water to the N aquifer is restricted to the southeast edges of the mesa.

The current climate in the area is semiarid; the mean annual precipitation (MAP) is <300 mm in much of the area but as much as 320 mm in areas >1800 m in elevation. The mean annual temperature is  $\sim 10^\circ\text{C}$  in the Shonto area. Vegetation consists of grass shrub at altitudes below 1670 m, piñon-juniper between 1670 and 2280 m, and pine forest above 2280 m [Cooley *et al.*, 1969]. During the late Pleistocene the temperatures were  $5^\circ\text{--}6^\circ\text{C}$  cooler than today, but during the mid-Holocene, summer temperatures were  $2^\circ\text{--}4^\circ\text{C}$  warmer than presently [Zhu *et al.*, 1998].

### 3. Sample Collection and Analytical Results

In this study, water samples were collected from production wells and windmills for the analysis of  $^{14}\text{C}$ ,  $\delta^{13}\text{C}$ ,  $^3\text{H}$ ,  $\delta\text{D}$ ,  $\delta^{18}\text{O}$ , K, Na, Ca, Mg, Al,  $\text{SiO}_2$ , Cl,  $\text{SO}_4^{2-}$ ,  $\text{NO}_3^-$ , and  $\text{NO}_2^-$ . The pH, alkalinity, specific conductance, dissolved oxygen (DO), and temperature were determined in the field. Pure  $\text{CO}_2$  gas for  $^{14}\text{C}$  analysis was prepared by the Environmental Isotope Lab-

**Table 1.** Symbols, Notations, Acronyms, and Definitions

Symbols	Definitions
TDIC	total dissolved inorganic carbon, includes $\text{HCO}_3^-$ , $\text{CO}_3^{2-}$ , $\text{H}_2\text{CO}_3^0$ , and metal carbonate and bicarbonate complexes; TDIC values are calculated from alkalinity and field pH through speciation modeling in this study
TDS	total dissolved solids (mg/L)
$A$	measured $^{14}\text{C}$ activity of TDIC in groundwater samples
$A_0$	projected initial activity of the packet groundwater before having undergone any radioactive decay but having undergone all mixing and reactions; $A_0$ is obtained from inverse geochemical modeling
$R$	recharge, either as volumetric recharge to the aquifer ( $L^3/T$ ) or specific recharge ( $L/T$ )
$K$	hydraulic conductivity ( $L/T$ )
pmc	percent modern carbon as the measured $^{14}\text{C}$ activities of the samples, with reference to the NIST HOxI standard
$n_e$	effective porosity

oratory (EIL) of the University of Waterloo, and radiocarbon activities were analyzed by the Rafter Radiocarbon National Laboratory of New Zealand. The  $^{14}\text{C}$  activities were measured using accelerator mass spectrometry and reported as percent modern carbon (pmc) based on the National Institute of Standards and Technology (NIST) (HOxI) oxalic acid standard. Analyses for  $^{13}\text{C}$ , D,  $^{18}\text{O}$ ,  $^{34}\text{S}$ , and enriched  $^3\text{H}$  were conducted at the University of Waterloo. The reported uncertainties are  $<0.5\%$  for  $^{14}\text{C}$  and  $<0.3\%$  for  $\delta^{13}\text{C}$ . Enriched  $^3\text{H}$  was counted using liquid scintillation counters with a detection limit of  $\sim 0.8$  tritium units (TU, 1 TU = 3.2 pCi/L) and a precision of about  $\pm 0.3$  TU. The results for  $^{13}\text{C}$ , D, and  $^{18}\text{O}$  are expressed in conventional  $\delta\%$  notation relative to Pee Dee belemnite (PDB) and VSMOW standards, respectively.

The  $^{14}\text{C}$  data as well as other chemical and isotopic data for N aquifer water were also collected by Wickham [1992] and Lopes and Hoffman [1997]. These data are listed together with those from this study in Tables 2 and 3. All data in Tables 2 and 3 are included in the analyses below. Figure 2 shows the locations of samples collected.

## 4. Synthesis and Interpretation of Chemical and Isotopic Data

### 4.1. Major Ion Geochemistry

The evolutionary path of groundwater geochemistry is relatively clear in the N aquifer. Groundwater in the confined portion of the N aquifer is predominantly of the  $\text{Na}^+\text{-HCO}_3^-$  type (Figure 4). In the Shonto area the groundwater is of the  $\text{Ca}^{2+}\text{-Mg}^{2+}\text{-HCO}_3^-$  type, with a pH of 7.5–8.0. Groundwater in the recharge area is also characterized with low  $\text{SO}_4^{2-}$  and low TDS. Shortly after groundwater enters into the confined portion of the aquifer,  $\text{Ca}^{2+}$  and  $\text{Mg}^{2+}$  concentrations decrease sharply, while  $\text{Na}^+$  concentrations increases proportionally. Thus, along the direction of flow, groundwater becomes  $\text{Na}^+\text{-HCO}_3^-$ -type water. This trend continues as groundwater flows downgradient to the southwest, and pH increases to up to 10. Wickham [1992] showed that the relationship between  $\text{Na}^+$  and  $\text{Ca}^{2+}$  and  $\text{Mg}^{2+}$  concentrations can be explained by Na-Ca and Na-Mg cation exchange between water and, presumably, clay minerals. The  $\text{Na}^+\text{-SO}_4^{2-}\text{-Cl}^-$  or  $\text{Na}^+\text{-SO}_4^{2-}$ -type waters are found near the southeastern part of the Black Mesa and are associated with increased TDS. The increased TDS,  $\text{SO}_4^{2-}$ , and  $\text{Cl}^-$  are believed to be a result of the leakage from the D aquifer [Dulaney, 1989; Wickham, 1992; Lopes and Hoffman, 1997].

Total dissolved inorganic carbon (TDIC) in groundwater first decreases from  $\sim 2.2$  mmol/L in the Shonto area to  $\sim 1.2$ – $1.7$  in the area  $\sim 15$  km southeast of Shonto (Table 2). TDIC

subsequently increases to  $\sim 2$  mmol/L in the center of the basin and increases further toward the southwest. Solubility and speciation calculations using WATEQ [Trusdell and Jones, 1974] show that N aquifer groundwater is close to saturation with respect to calcite, undersaturated with respect to gypsum, supersaturated with quartz, but undersaturated with respect to amorphous silica.

### 4.2. Stable Isotope D and $^{18}\text{O}$

The  $\delta\text{D}$  and  $\delta^{18}\text{O}$  data show two distinct groups (Figure 5). Samples from the unconfined aquifer, which generally have Holocene ages ( $^{14}\text{C}$  ages less than ca. 11 ka, see below), have heavier oxygen and hydrogen isotopes; samples from the confined aquifer, which generally have Pleistocene ages (greater than ca. 11 ka), have depleted  $\delta^{18}\text{O}$  and  $\delta\text{D}$ . The samples in Figure 5 that do not fall into their respective groups are mixtures of old and young water, as indicated by their locations and tritium contents (Table 3). This distinct grouping was interpreted to be the result of paleoclimatic changes that occurred during late Pleistocene and Holocene [Zhu et al., 1998]. During cooler and more humid climates, precipitation was depleted in  $\delta^{18}\text{O}$  and  $\delta\text{D}$  with respect to recent waters [Merlivat and Jouzel, 1979]. The samples from the unconfined aquifer show deviations from the global meteoric water line (GMWL) [Craig, 1961] and the local mean water line [Coplen, 1992], which likely reflect the effects of evaporative processes in the arid climate characteristic of Black Mesa.

### 4.3. Carbon Isotopes and Tritium

Measurable amounts of tritium were found in some wells from the unconfined N aquifer or at the periphery of the confined aquifer (Table 3). The presence of tritium in these samples indicates mixing with young water ( $<50$  years) in these wells. No measurements of  $\delta^{13}\text{C}$  for soil  $\text{CO}_2$  gas were made in Black Mesa;  $^{14}\text{C}$  measurements of two soil samples were, however, reported by Lopes and Hoffman [1997]. The  $^{14}\text{C}$  activities from the soil samples were 45 and 97 pmc, respectively. The measured high  $^{14}\text{C}$  activities in soil samples are consistent with soil samples in other semiarid areas, for example, the Upper San Pedro basin (66 and 88.3 pmc [Robertson, 1992]) and the Tucson basin ( $<0.67$  to 66 pmc, average of 24 pmc for nine samples [Wallick, 1976]). No  $\delta^{13}\text{C}$  measurements were made for these pedogenic calcites. The  $\delta^{13}\text{C}$  values for carbonate in N and D aquifer sandstone outcrops range from  $-8.3$  to  $+1.8\%$  (mean and standard deviation of  $3.2\% \pm 3.7\%$ ,  $n = 5$  [GeoTrans, unpublished report, 1993]). No measurements of  $^{14}\text{C}$  were made on calcite cements in the N aquifer.

**Table 2.** Chemical Data of N Aquifer Groundwater Samples

Well/Sample Names	References <sup>a</sup>	Temperature, °C	pH (field)	TDIC, <sup>b</sup> mmol/L	DO, mg/L	Ca <sup>2+</sup> , mmol/L	Mg <sup>2+</sup> , mmol/L	K <sup>+</sup> , mmol/L	Cl <sup>-</sup> , mmol/L	Na <sup>+</sup> , mmol/L	SO <sub>4</sub> <sup>2-</sup> , mmol/L	SiO <sub>2</sub> , mmol/L	NO <sub>3</sub> <sup>-</sup> , mmol/L
NAVAJO NAT.M.	2	16.7	8.1	2.0707	7.7	0.9207	0.1646	0.0358	0.1128	0.2218	0.0000	0.2929	0.0116
NAVAJO NAT.M.	1	13.4	8.1	2.1004	8.0	0.8483	0.1090	0.0274	0.0762	0.1509	0.0284	0.0925	0.3020
Solar Well	2	13.1	7.9	1.9456	6.4	0.8508	0.1522	0.0384	0.1410	0.2262	0.0000	0.2796	0.0210
08T-510	2	12.9	7.9	3.6043		1.5071	0.2633	0.0256	0.0564	0.2958	0.0000	0.2380	0.0884
Shonto PM1	2	13.8	7.5	2.2113	8.2	1.3025	0.2798	0.0435	0.5641	0.2914	0.1718	0.2580	0.0605
Shonto PM2	2	13.7	7.8	2.4138	7.2	1.3099	0.2880	0.0435	0.4231	0.2871	0.1572	0.2613	0.0577
Shonto PM4	3	13.5	7.9	2.2315	6.9	1.0729	0.2345	0.0384	0.3103	0.2958	0.1562	0.2465	0.0000
Shonto Sch #2	1	13.8	7.8	2.3569	8.6	1.2433	0.1950	0.0308	0.2708	0.2447	0.1197	0.3194	1.1209
02K-300	2	13.9	8.2	2.5993	11.1	1.1328	0.2386	0.0435	0.3385	0.2479	0.1384	0.2446	0.0416
02T-518A	2	17.9	8.1	2.6145	6.4	0.7386	0.2304	0.0409	0.2257	0.5524	0.0614	0.2613	0.0169
01K-225	2	14.7	7.6	4.4723	2.6	1.5046	0.3868	0.0563	0.2821	0.5176	0.3862	0.2047	0.0455
02P-512	2	15.5	8.1	2.7183	10.8	0.9482	0.1193	0.0230	0.1410	0.2218	0.0635	0.2363	0.0295
08T-522	2	17.9	7.4	6.4989	5.9	1.8564	1.0286	0.0870	0.3667	2.4532	1.0410	0.1947	0.0113
Kayenta Sch 2	2	17.5	8.4	1.3946	7.3	0.8483	0.3168	0.0358	0.1128	1.0004	0.6454	0.2679	0.0132
Kayenta Sch 2	1	16.2	8.2	2.1966	7.8	1.1622	0.3143	0.0323	0.0928	1.1225	0.7683	0.2879	0.3106
9Y-92	1	14.7	8.1	4.0460	13.8	3.1623	1.8844	0.0834	0.3244	2.6181	5.0803	0.1765	1.3422
9K-215	1	15.3	8.5	3.9547	4.3	1.2485	0.8344	0.3274	8.7606	16.4177	4.4348	0.0882	4.6178
Tuba City Sch PM5	1	16.6	8.0	1.5977	6.8	0.6013	0.1531	0.0281	0.1250	0.4050	0.1093	0.2479	0.5783
Tuba City 3	3	16.5	7.9	1.6098	6.6	0.5739	0.1687	0.0256	0.1241	0.3480	0.0781	0.1807	0.0000
08T-541	2	15.3	8.7	2.0018	6.5	0.2470	0.1070	0.0793	0.1128	1.6398	0.0989	0.2430	0.0058
Kayenta #5	2	22.9	8.6	1.9459	7.1	0.1747	0.0535	0.0332	0.0846	1.9617	0.0708	0.2530	0.0052
Kayenta NUTA6	2	25.5	8.6	1.7483	5.9	0.0998	0.0288	0.0307	0.1128	2.2706	0.0541	0.2413	0.0079
Kayenta NTUA4	2	21.0	8.7	2.2667	9.9	0.1447	0.0535	0.0332	0.0846	2.0922	0.1280	0.2313	0.0048
Kayenta NTUA4	3	18.0	9.1	2.0996	6.4	0.1272	0.0453	0.0332	0.1382	2.1749	0.2186	0.2136	0.0000
01K-214	2	16.6	8.1	2.1319	6.5	0.7835	0.3662	0.0614	0.1410	0.4306	0.1083	0.2513	0.0352
Red Lake NTUA1	3	17.0	8.4	1.5405	6.8	0.3992	0.1399	0.0281	0.0451	0.6090	0.0281	0.2136	0.0000
Red Lake NTUA1	2	16.7	8.8	1.2774	8.1	0.4466	0.1481	0.0281	0.0564	0.5872	0.0239	0.2213	0.0155
Red Lake Sch PM1	1	16.8	8.4	1.5135	7.7	0.4518	0.2139	0.0486	0.0186	0.1357	0.0176	0.0736	0.4334
NAV9	3	32.0	8.8	1.3603	5.5	0.0923	0.0012	0.0153	0.0451	1.4354	0.0302	0.3286	0.0000
NAV9	2	31.6	9.2	1.2151	5.7	0.0998	0.0000	0.0000	0.0564	1.3919	0.1457	0.3368	0.0535
NAV5	2	31.3	9.4	1.7356	6.3	0.0749	0.0000	0.0256	0.1128	2.5664	0.2394	0.3796	0.0678
NAV3	2	31.4	9.2	1.2971	6.2	0.0998	0.0000	0.0256	0.0564	1.6529	0.4685	0.3648	0.0593
NAV8	2	28.4	8.2	1.8716	6.8	0.7238	0.1646	0.0768	0.1129	2.9589	1.0830	0.3796	0.1178
NAV6	3	33.5	8.9	1.4950	4.8	0.0973	0.0012	0.0179	0.0536	1.6094	0.0687	0.3779	0.0000
Forest Lake NTUA	1	28.9	9.6	1.9376	5.7	0.0235	0.0021	0.0017	0.2581	3.5250	0.3893	0.1492	0.2499
Forest Lake	3	29.0	9.4	2.1041	5.1	0.0274	0.0049	0.0179	0.3667	4.2628	0.6246	0.3451	0.0000
Kitsille	1	28.7	9.8	2.7831	5.3	0.0235	0.0041	0.0071	0.1295	4.1752	0.0459	0.3971	0.4398
Chilchinbito PM3	1	20.2	9.7	3.0945	8.1	0.0157	0.0000	0.0109	0.0578	3.6790	0.0366	0.3804	0.4062
Chilchinbito NTUA1	3	21.0	9.5	3.4065	5.2	0.0175	0.0016	0.0128	0.0705	4.0018	0.0396	0.2793	0.0000
8T-518	1	16.4	9.5	5.0320	2.5	0.0146	0.0049	0.0133	0.8645	6.4037	0.2176	0.0526	0.3691
10R-111	1	16.3	8.5	1.3454	9.5	1.7298	0.4156	0.1265	2.4963	48.0834	22.0701	0.0861	0.3020
3M-156	1	16.5	9.6	3.6099	0.5	0.0168	0.0012	0.0113	1.1762	7.2382	0.9088	0.1618	0.0236
Rocky Ridge	3	27.0	9.5	1.8503	5.6	0.0102	0.0008	0.0102	0.0367	2.3489	0.0573	0.3451	0.0000
Rocky PM2	1	27.4	9.6	1.8679	4.9	0.0041	0.0000	0.0091	0.0291	2.3443	0.0519	0.2857	0.4476
Hard Rocks	3	29.5	9.2	3.1968	3.8	0.0190	0.0025	0.0179	1.1283	6.0897	0.7704	0.3779	0.0000
Pinon PM6	3	27.0	10.0	2.8979	5.3	0.0133	0.0000	0.0023	0.0815	4.4661	0.0421	0.2396	0.5112
Pinon	1	26.5	10.2	2.7885	4.3	0.0137	0.0004	0.0102	0.1015	4.7847	0.0468	0.4601	0.0000
Hotevilla Sch 2	1	26.0	9.8	2.0680	5.6	0.0140	0.0000	0.0105	0.0299	2.8234	0.0482	0.3952	0.3663
2nd Mesa	1	20.2	9.7	4.7645	0.7	0.0090	0.0000	0.0125	0.1673	6.0992	0.1478	0.2563	0.0023
Hopi High Sch3	1	20.3	8.8	6.5203	0.1	0.0387	0.0099	0.0199	7.1644	15.0924	0.8276	0.0841	0.0064
Low Mtn PM2	1	20.3	9.2	6.4637	0.2	0.0355	0.0099	0.0087	5.6413	13.6891	0.7048	0.1870	0.0157

<sup>a</sup>1, Wickham [1992]; 2, this study; 3, Lopes and Hoffman [1997].<sup>b</sup>TDIC calculated from WATEQ/NETPATH.

#### 4.4. The <sup>14</sup>C Age Corrections

A voluminous literature exists on correcting <sup>14</sup>C groundwater ages [e.g., Vogel, 1967, 1970; Ingerson and Pearson, 1964; Pearson, 1965; Pearson and Hanshaw, 1970; Tamers, 1967a, 1967b, 1975; Mook, 1972, 1976, 1980; Geyh, 1970, 1972; Fritz et al., 1978; Wigley, 1975; Wigley et al., 1978; Fontes and Garnier, 1979; Fontes, 1983, 1992; Plummer et al., 1990, 1991]. However, none of the published models appear to be adequate for applications to Black Mesa. Hence we devised a different correction strategy and a new correction model by (1) dividing the flow path into two segments and making corrections separately for each segment and (2) using a three carbon sources mixing

model rather than two as in all previous models. In the following discussion, the term correction approach is used to refer to the general method. For example, mass balances based on major ions, on  $\delta^{13}\text{C}$ , or on a combination of both are all correction approaches. A correction model, on the other hand, refers to the mathematical formulae that represent a specific set of mass transfer reactions. Many specific models have been proposed following a given approach such as a mass balance on major ions. The correction strategy refers to the overall application of approaches and models to a field situation.

The first flow path segment encompasses water (snow melt) passing through the soil zone and reaching wells that are close

**Table 3.** Isotopic Data of N Aquifer Groundwater Samples

Well/Sample Names	References <sup>a</sup>	Sampling Date	$\delta D$ VSMOW	$\delta^{18}O$ VSMOW	$\delta^{13}C$ PDB	$^{14}C$ , pmc	$^3H$ , TU
NAVAJO NAT.M.	2	Aug. 25, 1996	-95.07	-12.17	-10.5	55.5	<0.8
NAVAJO NAT.M.	1	1990	-94	-12.6	-12	72.9	
Solar Well	2	Aug. 27, 1996	-89.03	-11.64	-9.6	51.4	<0.8
08T-510	2	Aug. 27, 1996	-86.41	-11.7	-8.9	90.7	11.5
Shonto PM1	2	Aug. 27, 1996	-85.79	-10.76	-7.7	63.5	1.2
Shonto PM2	2	Aug. 27, 1996	-86.1	-10.7	-7.7	63.3	0.8
Shonto PM4	3	Feb. 25, 1993	-87.6	-11.03	-7.7	59.6	0.34
Shonto Sch #2	1	1990	-80	-10.9	-7.9	64.4	
02K-300	2	Aug. 27, 1996	-83.81	-10.37	-7.1	60.6	<0.8
02T-518A	2	Aug. 27, 1996	-81.84	-10.46	-6.8	59.7	<0.8
01K-225	2	Aug. 27, 1996	-78.22	-9.56	-7.8	55.6	<0.8
02P-512	2	Aug. 27, 1996	-86.27	-10.76	-8.3	63.2	<0.8
08T-522	2	Aug. 27, 1996	-84.08	-9.59	-10.1	68.3	11.4
Kayenta Sch 2	2	Aug. 27, 1996	-88.82	-11.03	-8.9	21	<0.8
Kayenta Sch 2	1	1990	-80	-10.5	-8.3	32	
Tuba City Sch PM5	1	1990	-68	-9.7	-7.4	47.2	
Tuba City 3	3	Feb. 25, 1993	-78	-9.38	-7.5	62.4	0.28
08T-541	2	Aug. 27, 1996	-108.1	-14.21	-11.2	2.8	<0.8
Kayenta 5	2	Aug. 27, 1996	-113.7	-14.67	-10.1	4.8	<0.8
Kayenta NUTA6	2	Aug. 27, 1996	-111.8	-14.26	-9.1	5.7	<0.8
Kayenta NTUA4	2	Aug. 27, 1996	-109.6	-13.88	-10.4	4	<0.8
Kayenta NTUA4	3	Feb. 11, 1993	-111	-14.43	-9.5	2.4	<0.09
01K-214	2	Aug. 27, 1996	-95.46	-12.46	-8.2	34.4	<0.8
Red Lake NTUA1	3	Mar. 24, 1993	-103	-13.16	-7.9	24.8	0.13
Red Lake NTUA1	2	Aug. 27, 1996	-104.1	-13.14	-9.1	23.3	<0.8
Red Lake Sch PM1	1	1990	-104	-13.4	-9.8	26.4	
NAV9	3	Apr. 21, 1993	-101	-13.35	-8.7	7	<0.09
NAV9	2	Oct. 21, 1992	-97	-13.4	-9.6	10.8	
NAV5	2	Oct. 21, 1992	-100	-13.4	-10.5	14.3	
NAV3	2	Oct. 21, 1992	-101	-13.5	-9.7	7.5	
NAV8	2	Mar. 24, 1997	-93.4	-12.18	-11.28	48.79	
NAV6	3	Apr. 21, 1993	-104	-13.55	-9.1	9.8	<0.09
Forest Lake NTUA	1	1990	-105	-14.1	-7.9	6.8	
Forest Lake	3	Aug. 9, 1995	-107	-13.86	-8.1	1.1	
Kitsille	1	1990	-98.00	-13.10	-7.10	3.0	
Chilchinbito PM3	1	1990	-96	-13	-7.3	7.2	
Chilchinbito NTUA1	3	Mar. 10, 1993	-102	-13.25	-6.6	0.9	<0.09
8T-518	1	1990	-101.00	-13.40	-6.60	11.4	
10R-111	1	1990	-98.00	-13.35	-6.60	13.8	
3M-156	1	1990	-98.00	-13.10	-9.50	4.6	
Rocky Ridge	3	Mar. 25, 1993	-108	-14.19	-8.8	2.7	
Rocky PM2	1	1990	-108	-13.9	-9.6	1.9	
Hard Rocks	3	May 12, 1993	-104.00	-13.66	-6.80	1.9	<0.09
Pinon PM6	1	1990	-94.00	-12.90	-8.50	7.2	
Pinon	3	Mar. 18, 1993	-99.70	-13.00	-7.10	0.9	<0.09
Hotevilla Sch 2	1	1990	-107	-13.7	-8.3	0.6	
2nd Mesa	1	1990	-100.00	-13.10	-7.50	1.5	
Hopi High Sch3	1	1990	-99.50	-13.81	-7.20	3.8	
Low Mtn PM2	1	1990	-99.00	-13.50	-6.80	2.0	

<sup>a</sup>1, Wickham [1992]; 2, this study; 3, Lopes and Hoffman [1997].

to the Shonto area. In this area, where all of the wells are in the unconfined zone of the aquifer, high  $^{14}C$  activities are observed. For this segment a mass balance–mass transfer model was used to reconstitute the major ions and proportions of mineral- and soil gas–derived carbon in groundwater. The initial radiocarbon activities for the samples were calculated from mixing ratios of soil gas  $CO_2$  and pedogenic carbonate.

The second segment of the flow path is largely in the confined aquifer. Travel time of a packet of water between an “initial” well and a “final” well was calculated following the mass balance model of Wigley *et al.* [1978]. The isotopic dilution from “dead” carbon or calcite cement in the sandstones is taken into account as a third carbon source in addition to soil gas and pedogenic carbonate that provided carbon along the first segment. Thus age correction applied to wells in the basin

is essentially a three–end-member mixing model. The age of the water from a final well is the sum of the travel time along the second segment and the age calculated for the initial well.

**4.4.1. Ages of water in the recharge area.** Mass transfer calculations following Garrels and Mackenzie [1967] were performed for the wells in the recharge areas. The components Na, Ca, Mg, K, C, S, Cl, and Si were used to reconstruct the sources of groundwater constituents. The starting solution had the average chemical concentrations of eight snow samples analyzed by Dulaney [1989]. The inverse mass balance modeling calculated ratios of soil  $CO_2$  gas– and soil carbonate mineral–derived carbon (Table 4). These ratios were then used to calculate the initial activities ( $A_0$  in Table 4) for age corrections. Soil  $CO_2$  was assumed to have a 100% modern carbon. The activity of pedogenic carbonate was taken as the average

of the two available measurements (71% modern) reported by *Lopes and Hoffman* [1997].

The correction approach here is essentially that of *Tamers* [1975], which is based on major ion mass balance. At Black Mesa the lack of  $\delta^{13}\text{C}$  measurements for soil  $\text{CO}_2$  and calcite precludes the use of  $^{13}\text{C}$ -based approach for corrections. However, the set of reactions used in the mass transfer model differs from the set used in the *Tamers* [1975] model or other previous major ion mass balance models [*Plummer et al.*, 1990; *Fontes and Garnier*, 1979] in that it includes both plagioclase weathering and ion exchange. Plagioclase is abundant in the Navajo Sandstone [*Dulaney*, 1989], and plagioclase weathering should be expected in the soil zone. It should be noted that different mass balance models can be constructed using other mineral phases than those chosen here. For example, the use of anorthite instead of plagioclase  $\text{An}_{38}$  would result in slightly smaller calculated mineral/soil gas carbon ratios. No feldspar compositional data are available for Navajo sandstone. The choice of  $\text{An}_{38}$  is based on convenience because it is in the NETPATH database [*Plummer et al.*, 1991]. The lack of feldspar composition data constitutes a source of errors for age correction, but these errors are quite small.

**4.4.2. Calculation of travel times along segment 2.** Travel times from the Shonto recharge area to the downgradient wells in the center and southwest of the basin were calculated with the aid of the mass balance program NETPATH [*Plummer et al.*, 1991]. Changes in TDIC along flowpaths were interpreted as the result of precipitation or dissolution of calcite cement. Degassing of  $\text{CO}_2$  or decomposition of organic matter is unlikely to be significant in the confined portion of the N aquifer. NETPATH treats the dissolved carbon as having the same isotopic signature as the minerals, but precipitation of carbonate minerals results in isotopic fractionation that is described by the Rayleigh distillation process [*Wigley et al.*, 1978; *Plummer et al.*, 1991]. Differences between the observed  $\delta^{13}\text{C}$  and computed  $\delta^{13}\text{C}$  were reconciled by adjusting the amount of carbon engaged in carbon isotopic exchange between aqueous carbonate species and calcite. It is known that the diffusion of isotopes in solids at low temperatures is too slow to be signif-

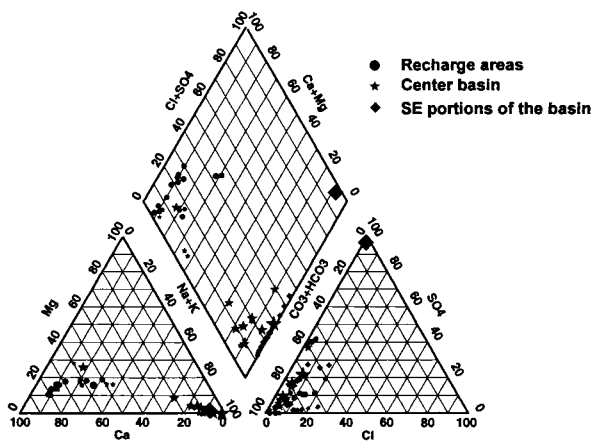


**Figure 4.** Piper diagram shows the groundwater major ion proportions. Ca-Mg- $\text{HCO}_3^-$ -type groundwater from the recharge area quickly evolves into Na- $\text{HCO}_3^-$ -type groundwater in the center of the basin. In the SE part of the basin, leakage from the overlying D aquifer results in high  $\text{SO}_4^{2-}$  concentrations. Symbol sizes are proportional to total dissolved solids.

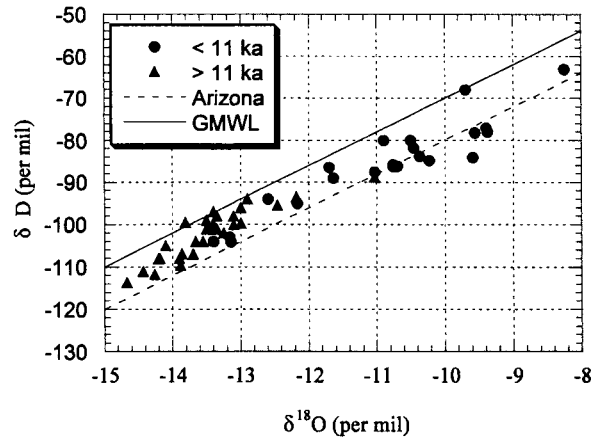


**Figure 5.** The  $\delta^{18}\text{O}$  and  $\delta\text{D}$  data (VSMOW) for  $^{14}\text{C}$  dated N aquifer water. The Arizona local meteoric water line ( $\delta\text{D} = 8\delta^{18}\text{O} + 0$ ) is from *Coplen* [1992]. Global meteoric water line (GMWL) is from *Craig* [1961].

icant [*Mook*, 1980]. *Plummer et al.* [1991] treated isotopic exchange in NETPATH as precipitation and dissolution of equal amounts of carbonate (recrystallization) with isotopic fractionation accompanying precipitation according to the Rayleigh distillation process. The  $^{13}\text{C}$  fractionation factors of *Mook* [1980] were used in our calculations. NETPATH defines the  $^{14}\text{C}$  fractionation factors as twice those for  $^{13}\text{C}$ .

Precipitation of quartz, illite, or kaolinite, the dissolution of gypsum and plagioclase, and Ca-Na exchange are inferred from the modeling (Table 5). Although these reactions are needed to interpret the increases of  $\text{Na}^+$ ,  $\text{SO}_4^{2-}$ ,  $\text{SiO}_2(\text{aq})$ , and  $\text{K}^+$  and decrease of  $\text{Ca}^{2+}$  in downgradient wells, the noncarbonate reactions do not affect the calculation of carbonate reaction and age corrections. The carbon isotopes are solely constrained by the TDIC and  $\delta^{13}\text{C}$  values.

The final corrected age for each well was derived by adding the calculated travel time along segment 2 to the age calculated along segment 1 for the upstream well that was used to define the “initial” ion concentration for the NETPATH simulation. Figure 6 shows the corrected ages. No corrections were attempted for samples that had high concentrations of  $\text{Cl}^-$ ,  $\text{SO}_4^{2-}$ , and  $\text{Na}^+$ , indicative of significant mixing from the D aquifer. The amounts of corrections to the apparent ages are shown in Figure 7.

**4.4.3. Discussion of the corrected ages.** Although our approach to age correction is within the established practice of using major ion and  $\delta^{13}\text{C}$  mass balance to reconstitute proportions of carbon from different sources, it is innovative in its application to a field situation. First, we used distinct models for wells in the recharge area and those in downgradient areas. In nearly all previous work, a single model was used throughout the aquifer, with the effect of all chemical reactions together, including those occurring in both the unsaturated and saturated zones. Chemical inversion in such a manner could misappropriate mass transfer reactions that occur along different segments of the flow path, introducing unnecessary uncertainties and leading to larger corrections than warranted. Dividing the flow path into two segments minimizes the uncertainties from the chemical and isotopic assumptions for the unsaturated zone, where processes are complex and understanding is poor. Corrected ages for the short paths that

**Table 4.** Modeled Mass Transfer Reactions From Snowmelt to Groundwater in Wells in the Unconfined Area<sup>a</sup>

Well Names	NaCl	KCl	Gypsum	An <sub>38</sub>	Na-Ca Exchange	K-Mg	Calcite	MgCO <sub>3</sub>	CO <sub>2</sub>	Fraction of Mineral C	Calculated A <sub>0</sub>
NAVAJO NAT.M	0.1047	0.0000	0.0000	0.1118	-0.0176	-0.0152	0.8804	0.1769	0.9882	0.5106	85
NAVAJO NAT.M.	0.0680	0.0000	0.0223	0.0358	-0.0241	-0.0110	0.8105	0.1171	1.1430	0.4426	87
Solar Well	0.1329	0.0000	0.0000	0.1067	-0.0073	-0.0165	0.8021	0.1658	0.9525	0.4975	86
08T-510	0.0483	0.0000	-0.0061	0.0909	0.0000	-0.0101	1.5467	0.2705	1.8380	0.4938	86
Shonto PM1	0.5561	0.0000	0.1657	0.0985	0.0000	-0.0191	1.0779	0.2960	0.8122	0.6213	82
Shonto PM2	0.4150	0.0000	0.1511	0.0998	0.0000	-0.0191	1.0995	0.3042	0.9849	0.5815	83
Shonto PM4	0.3022	0.0000	0.1501	0.0953	0.0000	-0.0165	0.8651	0.2481	1.0931	0.4989	86
Shonto SCH 2	0.2627	0.0000	0.1136	0.1219	0.0000	-0.0127	1.0620	0.2049	1.0647	0.5375	84
02K-300	0.3304	0.0000	0.1323	0.0934	0.0000	-0.0191	0.9435	0.2548	1.3758	0.4610	87
02T-518A	0.2175	0.0000	0.0553	0.0998	-0.1303	-0.0178	0.7540	0.2453	1.5900	0.3822	89
01K-225	0.2740	0.0000	0.3802	0.0782	-0.0914	-0.0255	1.1648	0.4094	2.8729	0.3520	90
01K-214	0.1329	0.0000	0.1022	0.0959	-0.1129	-0.0280	0.7362	0.3913	0.7973	0.5288	85
02P-512	0.1261	0.0167	0.0615	0.0902	-0.0064	0.0000	0.8452	0.1081	1.7227	0.3529	90
Kayenta Sch 2	0.1047	0.0000	0.6394	0.1023	-0.4100	-0.0152	0.5849	0.3291	0.4818	0.6432	81
Kayenta Sch 2	0.0849	0.0000	0.7624	0.1112	-0.4781	-0.0134	0.8148	0.3249	1.0317	0.5188	85
08T-522	0.2700	0.0815	1.0450	0.0744	-1.0469	0.0000	1.7939	1.0163	3.4364	0.4481	87
Tuba City Sch PM5	0.1160	0.0000	0.1032	0.0959	-0.1083	-0.0114	0.5483	0.1616	0.8626	0.4443	87
Tuba City 3	0.1160	0.0000	0.0720	0.0690	-0.0884	-0.0101	0.5425	0.1760	0.8716	0.4448	87

<sup>a</sup>Modeled mass transfer reactions are in millimoles per liter. Positive numbers denote dissolution reactions and negative numbers precipitation reactions.

include the unsaturated zone may have uncertainties that are high in percentage but small in absolute value. In contrast, chemical reactions in the saturated zone are typically better constrained and hence the calculated travel time. Because the travel time along segment 2, in the saturated zone downgradient from the recharge area, constitutes the bulk of the calculated age, uncertainties in the overall ages are minimized.

Second, previously published correction models allow only two end-members for isotopic mixing. However, at Black Mesa at least three end-members are involved: soil CO<sub>2</sub>, pedogenic

calcite with high activities, and Navajo Sandstone calcite cement.

Third, models in the literature provide simple algebraic formulae for calculating the proportions of soil gas- and mineral-derived carbon. The mathematical simplicity comes at the expense of the need to assume a fixed set of mass transfer reactions. In reality, the mass transfer reactions are site-specific, depending on the aquifer mineralogy and other conditions. We would argue that no single correction models can be applied to all sites and that one should always develop

**Table 5.** Mass Transfer and Travel Time Calculated From Inverse Mass Balance Modeling for Wells in the Confined Area<sup>a</sup>

Well Name	Mass Transfer, mmol/L							Isotopic Exchange	Travel Time, k.y.
	Calcite	Gypsum	Kaolinite	Illite	Quartz	Na-Ca	An <sub>38</sub>		
08T-541	-0.0985	0.0705	-0.4019	0.0865	-0.8039	-0.6677	0.2482	0.22	26
Kayenta 5	-0.1545	-0.0284	-0.7248	0.0098	-1.4497	-0.7193	0.6010	0.55	21
Kayenta NTUA6	-0.3521	0.0257	-1.1466	0.0056	-2.2933	-0.7735	0.9243	0.95	18
Kayenta NTUA4	0.1663	0.0997	0.0494	0.0098	0.0988	-0.9703	0.0017	0.33	22
Kayenta NTUA4	-0.0193	0.1902	-0.1835	0.0098	-0.3671	-0.9583	0.1740	0.77	26
Red Lake NTUA1	-0.5785	-0.0003	-0.6215	0.0013	-1.2430	-0.0679	0.5197	1.32	4
Red Lake NTUA1	-0.8230	-0.0047	-1.1608	0.0013	-2.3216	0.0711	0.9331	0.80	7
Red Lake Sch PM1	-0.6054	-0.0107	-0.4722	0.0354	-0.9443	0.1030	0.3062	0.61	6
NAV9	-0.7584	0.0018	-1.0665	-0.0200	-2.1311	-0.3535	0.9316	1.16	15
NAV9	-0.8853	0.1173	-1.0909	-0.0030		-0.3319	0.9312	0.80	12
NAV5	-0.3648	0.1902	-1.0121	-0.0030	-2.1817	0.9344	0.8825	0.50	12
NAV3	-0.8032	0.4401	-0.5510	-0.0030	-1.1019	-0.5869	0.5299	0.76	16
NAV6	-0.6246	0.0403	-0.8956	-0.0158	-1.7912	-0.4766	0.8153	1.02	17
Forest Lake NUTA	-0.1813	0.3610	-1.1891	-0.0426		-1.3807	0.9869	1.60	14
Forest Lake	-0.0148	0.5964	-1.0860	-0.0158	-2.1720	-1.7628	0.9479	1.51	30
Chilchinbito PM3	0.9756	0.0080	0.2938	-0.0277	0.5875	-1.7885	-0.0754	1.15	14
Chilchinbito NTUA1	1.2875	0.0112	0.5239	-0.0243	1.0478	-2.0176	-0.2950	1.51	30
Rocky PM2	-0.2510	0.0236	-0.7619	-0.0303	-1.5238	-0.8810	0.6970	0.78	27
Hard Rocks	1.0779	0.7423	-0.4373	-0.0158	-0.8746	-2.8266	0.4655	1.61	24
Pinion PM6	0.7790	0.0132	-0.8597	-0.0418	-1.7193	-1.9205	0.7693	0.58	30
Pinion	0.6696	0.0185	-1.2731	-0.0286	-2.5463	-1.9607	1.1524	1.65	30
Hotevilla Sch 2	-0.0509	0.0195	0.0195	-0.0281	-1.6225	-1.0964	0.7744	1.36	35
Kayenta Sch2	-0.4559	0.6172	-0.4380	0.0141	-0.8760	-0.3064	0.3821	0.94	7
Kayenta Sch2	0.0777	0.7401	0.1178	0.0081	0.2357	-0.4936	-0.0252	1.20	3

<sup>a</sup>Two mass transfer models are listed here: precipitation of either illite or kaolinite. Positive numbers denote dissolution reactions and negative numbers precipitation reactions. Ten pmc for calcite cement was used for travel time calculations; 0 pmc would result in a few hundreds to <2000 years shorter travel time. Blank entries means no convergence. Components S, C, Si, K, Na, and Ca were used as constraints in modeling.

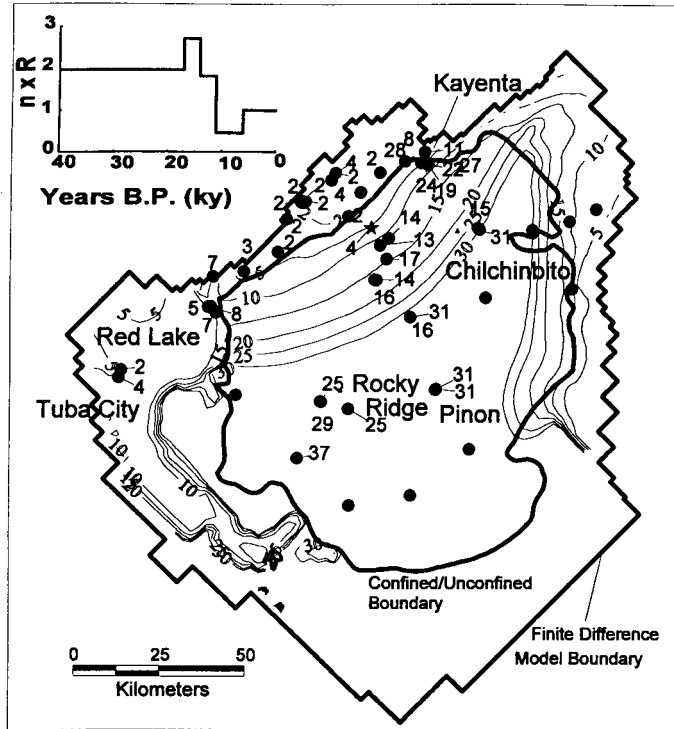


**Figure 6.** Comparison of corrected (circles) and simulated ages (contours). Insert shows recharge rates over the time used in the flow model, normalized by the calibrated value for modern recharge. The star represents newly acquired data after the simulation was performed. Modified from *Zhu et al.* [1998].

site-specific inverse mass balance models for the corrections. The availability of programs such as NETPATH, which can be used to formulate any correction “models” one desires, make this a feasible approach.

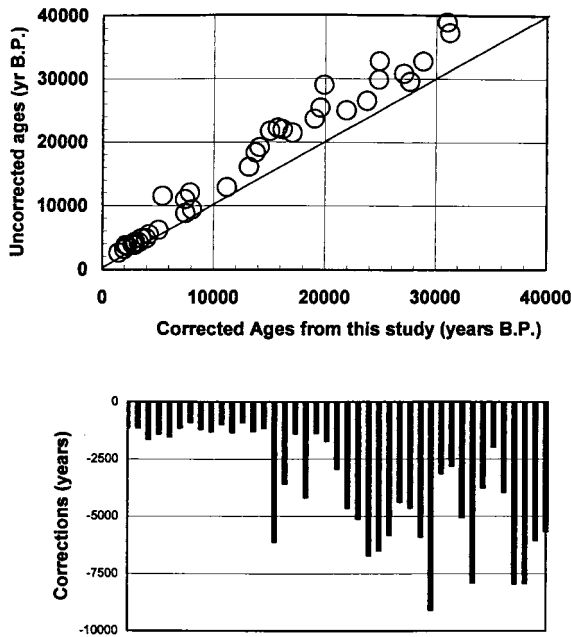


**Figure 7.** Comparison of apparent and corrected  $^{14}\text{C}$  ages. The apparent ages were calculated assuming decay from an initial activity of 100% modern carbon. The data were arranged in ascending order of ages.

## 5. Calibration of Recharge Rates

### 5.1. Calibration Strategy

It is well known that simulated heads are only sensitive to the ratios of recharge  $R$  and conductivity  $K$ . *Anderson and Woessner* [1992, p. 230] advised the use of known flow rates in model calibration in addition to heads, because “when calibrating a model, an increase in hydraulic conductivity creates the same effect on heads as a decrease in recharge making it possible to calibrate the model to head by adjusting either hydraulic conductivity or recharge.” This correlation has also been demonstrated by inverse modeling [*Sun, 1994; Poeter and Hill, 1997; Anderman et al., 1996; Portniaguine and Solomon, 1998*].

A unique solution or a narrower range of solutions to a given head distribution can only be obtained when either  $K$  or fluid flux, such as recharge or discharge, can provide independent constraints [*Sun, 1994*]. However,  $K$  can vary over a wide range in nature, making it often impractical to use it as a prior condition to reduce nonuniqueness. Laboratory measurements and pumping tests usually generate  $K$  values that span several orders of magnitude at a particular site. At Black Mesa the  $K$  values vary over 3–5 orders of magnitude for the Navajo sandstone [*Cooley et al., 1969*], which has relatively homogeneous lithology. Moreover, typical pumping tests only measure  $K$  for a few hundred meters around a well and therefore represent point measurements in a regional aquifer [*Phillips et al., 1989*]. Errors in  $K$  can also be introduced by pumping tests when well screens are completed in multiple hydraulic units [*Phillips et al., 1989*].

In temperate areas the constraint can sometimes be the recharge rate, which usually varies within a narrow range (for example, 15–30% of rainfall [*Lerner et al., 1990*]). On the other

hand, in semiarid and arid areas the recharge rate is very uncertain and can vary over orders of magnitude [Lerner *et al.*, 1990]. Discharge, as expected, is similarly difficult to measure in semiarid and arid regions, and the measurements may give a range so wide that they do not significantly narrow the range of parameters. Therefore, additional lines of independent evidence need to be introduced to constrain a value or a range of values of either  $K$  or  $R$  if either of these is to be used as an anchor point in the flow model.

The distribution of  $^{14}\text{C}$  groundwater ages in Figure 6 can be used to calculate an average advective velocity, which can be used, in turn, with an effective porosity  $n_e$  to constrain fluxes and hence recharge. This can be achieved by comparing simulated  $^{14}\text{C}$  ages from a numerical flow and transport model to observed  $^{14}\text{C}$  ages. Simulation of  $^{14}\text{C}$  transport is possible because during age correction the effects of mixing and geochemical reactions on the observed radiocarbon activities have already been accounted for. The simulated activities would be the radiocarbon activities if there were no chemical reactions along the flow path and if the transport of radiocarbon were only subject to radioactive decay and advective, dispersive, and diffusive processes. In other words, the transport of the reactive tracer,  $^{14}\text{C}$ , can be simulated using a two-step approach: (1) geochemical modeling to account for the chemical reactions and mixing and (2) transport modeling to simulate the advection-dispersion/diffusion and radioactive decay. In this manner, the problem of reactive transport of  $^{14}\text{C}$  is reduced to a nonreactive radioactive tracer transport problem.

During the calibration the recharge rates and hydraulic conductivity were adjusted iteratively until the simulated  $^{14}\text{C}$  ages and heads provided the best visual match to observations. The iteration followed a sequence similar to that proposed by Sun and Yeh [1990], although it was solved manually in this study. With a given effective porosity value the  $K$  and  $R$  are uniquely constrained. Because the calculated velocities are based on hydraulic gradients and hydraulic gradients are more sensitive to parameter values than heads,  $^{14}\text{C}$  ages provide a basis for finer tuning of calibrated input parameters.

## 5.2. Numerical Simulation of Flow and Transport

The calibration of recharge rates to the N aquifer and hydraulic conductivities was accomplished by developing a  $^{14}\text{C}$  transport model that is linked to the flow model. As a first approximation, a previously developed two-dimensional regional flow model was used (GeoTrans, unpublished report, 1987). This finite difference model had been developed using the modeling code MODFLOW [McDonald and Harbaugh, 1988] and had been calibrated to static water levels up to 1968 and pumping stresses up to 1994 (GeoTrans, unpublished report, 1994). The migration of  $^{14}\text{C}$  caused by advection, hydrodynamic dispersion, and radioactive decay was simulated using MODFLOWT, a finite difference flow and solute transport code [Duffield *et al.*, 1996]. Recharge rates were varied in the flow model until simulated  $^{14}\text{C}$  distribution best agreed with corrected  $^{14}\text{C}$  activities; hydraulic conductivities were adjusted in the same proportion as the recharge rates so that the model calibration to the water levels was maintained.

Because of the lack of constraints for dispersivity, sensitivity analysis was conducted by increasing the dispersivity by one order of magnitude (longitudinal dispersivity  $\alpha_L$  from 152 to 1520 m; transverse dispersivity  $\alpha_T$ , taken as one tenth of  $\alpha_L$ ). The differences in the simulation results were negligible. These results agree with Phillips *et al.* [1989], who used stochastic

theory to analyze the influence of hydrodynamic dispersion on  $^{14}\text{C}$  distribution in the nearby San Juan basin, northwestern New Mexico. Phillips *et al.* [1989] concluded that the effects of hydrodynamic dispersion do not exert a significant influence on the  $^{14}\text{C}$  distribution in large sedimentary aquifers with relatively homogenous lithology.

It should be noted that the  $^{14}\text{C}$  age correction, which is mainly based on mass balance of TDIC and  $\delta^{13}\text{C}$  between two wells, may already include the effects of dispersion if present. For example, a decrease of TDIC due to dispersion would have been attributed to calcite precipitation, and a decrease of  $\delta^{13}\text{C}$  due to dispersion would have been attributed to isotopic exchange with calcite cement. The above sensitivity and theoretical analysis merely pointed out that the dispersion effect should be negligible in the first place. Thus  $^{14}\text{C}$  age corrections based on the assumption of piston flow introduce only negligible errors for Black Mesa.

A specified flux boundary condition in the recharge was used. To compare the simulated  $^{14}\text{C}$  transport with groundwater ages, the corrected ages were converted to corrected  $^{14}\text{C}$  activities  $A'$  through the rearrangement of the radioactive decaying equation,

$$A' = A'_0 / \exp(t \ln 2 / 5730) \quad (1)$$

where  $A'_0$  stands for the nominal activity specified for the recharge in the transport model,  $t$  denotes the corrected ages (years) at the well point of interest, and the number 5730 is the half-life of  $^{14}\text{C}$  in years. The calculated activities  $A'$  correspond to the radiocarbon activities that would be observed if there were no mixing or chemical reactions along the flow path and if the transport of radiocarbon were subject only to radioactive decay plus the advective, dispersive, and diffusive transport processes. The assumption of a constant radiocarbon activity in recharge is a simplification because  $^{14}\text{C}$  content of the atmosphere has varied in the past 80 k.y. [Bard, 1997]. Starting from an assumed steady state condition at 65 ka, transient flow and transport was simulated from 65 ka to the present. A uniform effective porosity of 10% was used in the initial calibration of the transport model. Increasing the effective porosity from 10 to 15% resulted in the need to significantly increase the recharge to match the  $^{14}\text{C}$  age distribution (Table 6). Both 10 and 15% are considered conservative estimates of effective porosity based on existing data for this aquifer. Porosity determined by laboratory analysis of 24 cores from Navajo Sandstone ranges from 25 to 35%, and specific yield ranges from 18 to 29% for these cores [Cooley *et al.*, 1969]. With larger effective porosity, significantly higher recharge rates would be required to match the corrected  $^{14}\text{C}$  activities.

## 5.3. Simulation Results

The simulation showed that for a 15% effective porosity the average annual recharge for the past 6 k.y. is  $\sim 25 \times 10^6 \text{ m}^3/\text{yr}$  for all the N aquifer outcrops and  $11 \times 10^6 \text{ m}^3/\text{yr}$  in the Shonto area. For 10% effective porosity the average annual recharge for the past 6 k.y. is  $\sim 18 \times 10^6 \text{ m}^3/\text{yr}$  from all N aquifer outcrops and  $7 \times 10^6 \text{ m}^3/\text{yr}$  in the Shonto area. The hydraulic conductivities were adjusted to be 1.8 and 1.2 times higher than those in the original flow model for porosities of 15 and 10%, respectively, to maintain the calibration to static water levels at 1968. Significant variation of recharge rates over time is necessary to match the distribution of groundwater ages. These variations correlated well to inferred paleoclimatic changes in

**Table 6.** Comparison of Recharge Estimates From This Study to Previous Studies<sup>a</sup>

Areas	This Study, Effective Porosity of 10%	This Study, Effective Porosity of 15%	Previous Studies <sup>b</sup>			
			1	2	3, Effective Porosity of 10%	3, Effective Porosity of 15%
Shonto	7	11	6	7	1	2
Entire aquifer	18	25	17	12		

<sup>a</sup>Recharge estimates are in  $10^6 \text{ m}^3/\text{yr}$ .

<sup>b</sup>1, *Brown and Eychaner* [1988]; 2, GeoTrans (unpublished report, 1987); 3, *Lopes and Hoffman* [1997].

the late Pleistocene and Holocene [*Zhu et al.*, 1998]. A period of recharge rates 2–3 times higher than present rates from 31 to 11 ka followed by a period of reduced recharge from 6 to 11 ka was required to match the calculated  $^{14}\text{C}$  ages. The use of a constant recharge rate through time did not produce satisfactory calibration to  $^{14}\text{C}$  age distribution.

The inferred recharge rates in this study are derived from basal scale distribution of a radiometric tracer  $^{14}\text{C}$  in the saturated zone, and they represent the volumetric recharge flux that entered the entire groundwater system. This volumetric flux to the N aquifer can be converted to a specific recharge rate by dividing it by the surface area to which recharge is applied in the flow and transport model. The calibrated specific recharge rate calculated in this manner for the last 6 k.y. in the Shonto area is 19 mm/yr for simulations using 15% effective porosity and 13 mm/yr for simulations using 10% effective porosity.

## 6. Discussion

Our calibrated recharge rates can be checked independently with chloride data, which were not used in the calibration but which can be used to constrain recharge through the chloride mass balance (CMB) method [*Eriksson and Khunakasem*, 1969; *Allison and Hughes*, 1978; *Wood and Sanford*, 1995]. If we assume that for the last 6 k.y. the climate has been relatively stable and the mean annual precipitation and atmospheric deposition remained approximately constant, we can estimate the specific recharge from the  $\text{Cl}^-$  data and compare this to

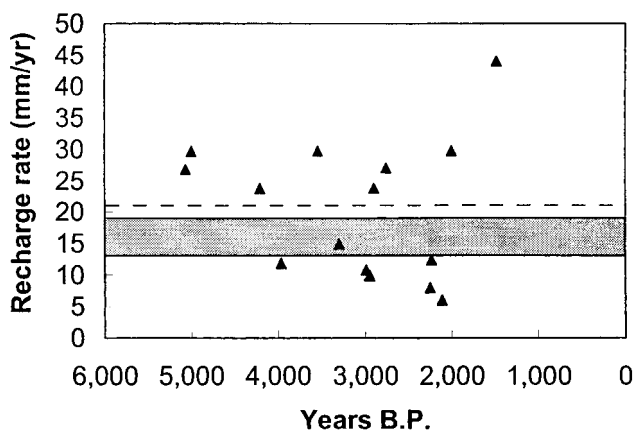


**Figure 8.** Comparison of recharge estimates for the last 6 k.y. from simultaneous calibration of ages and heads (gray box) and the chloride mass balance method (triangles). The dashed line at 21 mm/yr is the average of all chloride mass balance points. The gray box is bounded by calibrated average annual recharge rates with porosity range from 10 to 15%.

rates calculated from the linked flow and transport model. Using the average  $\text{Cl}^-$  concentration of  $8.18 \times 10^{-3} \text{ mmol/L}$  determined from eight snow samples from the Shonto area [*Dulaney*, 1989] and a mean annual precipitation of 305 mm/yr for the last 60 years (Western Regional Climate Center, available on the World Wide Web at [www.wrcc.dri.edu](http://www.wrcc.dri.edu)), the CMB method gives recharge rates that range from 5 to 20 mm/yr for most samples whose  $^{14}\text{C}$  ages are younger than 6 k.y., with an average of  $16 \pm 8 \text{ mm/yr}$ . Most recharge at Black Mesa occurs in the winter and spring months [*Cooley et al.*, 1969] so that the snow samples are a good approximation to the recharge. Summer  $\text{Cl}$  dry fallout accounts for 45% of total atmospheric  $\text{Cl}$  in Socorro, New Mexico, and the actual effective concentrations at Black Mesa are probably in the range of  $9\text{--}11 \times 10^{-3} \text{ mmol/L}$  (*F. Phillips*, personal communication, 2000). Using the higher end of this range gives an average estimated recharge of  $21 \pm 11 \text{ mm/yr}$  for the last 6 k.y. (Figure 8). These estimates again are based on assumptions that the average mean annual precipitation in the last 6 k.y. is close to the average of the last 60 years and that atmospheric deposition of  $\text{Cl}^-$  has been constant.

Our calibrated recharge is 51% higher than that of GeoTrans (unpublished report, 1987) and 35% higher than *Brown and Eychaner* [1988] when an effective porosity of 15% is used in our calibration. In the earlier studies, the Maxey-Eakin approach [*Maxey and Eakin*, 1949] was used to estimate recharge. Recharge rates equal to 3% of precipitation in the higher altitude Shonto area and 1% for other outcrops in lower altitudes were “assumed” without data support. The Maxey-Eakin method and its variants have been severely criticized by *Gee and Hillel* [1988], *Lerner et al.* [1990], and *Allison et al.* [1994]. Recent investigations show that recharge in semiarid and arid areas is episodic, and there is no linear correlation between annual precipitation and recharge [*Gieske*, 1992]. A low-intensity precipitation event in a period of high evapotranspiration results in less recharge than if precipitation occurs at a high intensity during a cold time of the year. Thus recharge in semiarid and arid areas may be more related to large, infrequent, extreme events than to the monthly, annual, or longer-term average of precipitation [*Gee and Hillel*, 1988; *Phillips*, 1994; *Simmers*, 1997]. Additionally, recharge in a model estimated from the Maxey-Eakin method strongly depends on the delineation of the recharge areas, which itself can carry large uncertainties.

With the same assumption of 15% porosity our recharge rate from the Shonto area is also 81% higher than values from *Lopes and Hoffman* [1997], who used  $^{14}\text{C}$  ages to estimate recharge rate to the N aquifer. They used hand-drawn isochrons to calculate water storage between  $^{14}\text{C}$  age isochrons. Their isochrons were drawn from 11 data points but lacked data control for the 10 k.y. isochron. In our distributed param-

eter flow and transport model approach, simulated  $^{14}\text{C}$  isochrons are not only controlled by  $^{14}\text{C}$  age data but also by flow patterns that are calibrated against hydraulic heads. Hence the calculated recharge rates are significantly more accurate and less subjective. Additionally, our approach fully utilizes aquifer geometry data.

As discussed above, the calibrated recharge rate in this study is highly sensitive to effective porosity. A decrease of porosity from 15 to 10% resulted in a decrease of 30% in the estimated recharge. Hence uncertainties in porosity result in nonunique estimates of recharge and hydraulic conductivity. The highly correlated problem of  $K$  and  $R$  is transformed to highly correlated parameter sets of  $K$ ,  $R$ , and  $n_e$  [Portniaguine and Solomon, 1998]. However, porosities of sediments or sedimentary rocks are typically less variable than recharge in semiarid and arid regions or hydraulic conductivity. Therefore the ranges and uncertainties of porosity still allow meaningful estimates of recharge and conductivity. Improved constraints can be obtained using multiple tracers.

## 7. Summary and Conclusions

1. This paper presents a general strategy for estimating average recharge to regional aquifers on the scale of thousands of years. It combines geochemical modeling to correct  $^{14}\text{C}$  groundwater ages and numerical modeling of  $^{14}\text{C}$  transport and groundwater flow. The strategy has broad applicability but has particular applications to arid and semiarid areas where estimating recharge rates is extremely difficult. The strategy can be a valuable tool for studies of regional aquifers to infer global environmental changes [e.g., Zhu et al., 1998] and for predicting performance of radioactive waste repositories in desert regions.

2. The strategy presented circumvents the numerous difficulties and assumptions associated with vadose zone tracer techniques. The derived recharge rates are basin-scale volumetric fluxes that enter the groundwater systems rather than local estimates of specific recharge that need to be generalized, extrapolated, and tied to the estimates of recharge areas and zonations. Thus they are better suited to be used in regional flow and transport models.

3. The calibration of the flow model to a distribution of ages is equivalent to calibrating the model to a lumped average of advective velocities. In general, flow models calibrated using hydraulic properties alone predict velocities that can be grossly inaccurate or carry large uncertainties [Duffield et al., 1990; NRC, 1990; Anderman et al., 1996]. Therefore simultaneous calibration to ages and heads is valuable for development of contaminant transport models, which typically take velocity fields from the flow model as input and in which velocities are often the most important factor to determine the direction and rate of contaminant transport.

4. The study demonstrates that geochemical and isotopic tracers can provide not only additional constraints on groundwater flow patterns but also constraints that are often independent from the hydraulic studies. The use of geochemistry in delineating groundwater flow patterns requires the knowledge of mass transport and geochemical reactions. This knowledge can be obtained through geochemical modeling, such as the inverse mass balance modeling employed in this study to correct  $^{14}\text{C}$  ages. Although such an approach introduces new variables that themselves have uncertainties, these uncertainties nevertheless can often be bounded and useful information

can be extracted. While a large amount of geochemical and isotopic data have become available in recent years, interpretations of these data have been mostly qualitative in groundwater studies. This study provides an example of how geochemical and isotopic data can be used to quantitatively delineate groundwater flow and transport.

**Acknowledgments.** I thank Ira Star, Rick Waddell, and Frank Schwartz for discussion and Jim Mercer and Kevin Johannesson for review of an earlier draft. Review comments from Peter Cook, Fred Phillips, and Jean Bahr helped to improve the manuscript significantly, and their time and interest is greatly appreciated. I am especially in debt to Jean Bahr, whose editing of the manuscript greatly improved its clarity. Assistance from Dana McClish in various aspects of this work is greatly appreciated. Financial support from NSF (EAR 0001020) and U.S. EPA is acknowledged, but the research does not reflect the views of the agencies.

## References

- Adar, E. M., and S. P. Neuman, Estimation of spatial recharge distribution using environmental and hydrochemical data, II, Application to Aravaipa Valley in Southern Arizona, U.S.A., *J. Hydrol.*, 97, 279–302, 1988.
- Allison, G. B., A review of some physical, chemical and isotopic techniques available for estimating groundwater recharge, *NATO ASI Ser., Ser. C*, 222, 49–72, 1988.
- Allison, G. B., and M. W. Hughes, The use of environmental chloride and tritium to estimate total recharge to an unconfined aquifer, *Aust. J. Soil Res.*, 16, 181–195, 1978.
- Allison, G. B., G. W. Gee, and S. W. Tyler, Vadoze-zone techniques for estimating groundwater recharge in arid and semiarid regions, *Soil Sci. Soc. Am. J.*, 58, 6–14, 1994.
- Anderman, E. R., M. C. Hill, and E. P. Poeter, Two-dimensional advective transport in groundwater flow parameter estimation, *Ground Water*, 34(6), 1101–1109, 1996.
- Anderson, M. P., and W. W. Woessner, *Applied Groundwater Modeling: Simulation of Flow and Advective Transport*, 381 pp., Academic, San Diego, Calif., 1992.
- Bard, E., Geochemical and geophysical implications of the radiocarbon calibration, *Geochem. News*, 93, 6–7, 1997.
- Brooks, R. J., D. N. Lerner, and A. M. Tobias, Determination of the range of prediction of a groundwater model which arises from alternative calibrations, *Water Resour. Res.*, 30, 2993–3000, 1994.
- Brown, J. G., and J. H. Eychaner, Simulation of five groundwater withdrawal projections for the Black Mesa area, Navajo and Hopi Indian Reservations, Arizona, U.S. Geol. Surv. *Water Resour. Invest. Rep.*, 88-4000, 51 pp., 1988.
- Campana, M. E., and E. S. Simpson, Groundwater residence times and recharge rates using a discrete-state compartment model and  $^{14}\text{C}$  data, *J. Hydrol.*, 72, 171–185, 1984.
- Cooley, M. E., J. W. Harshbarger, J. P. Akers, and W. F. Hardt, Regional hydrogeology of the Navajo and Hopi Indian Reservations, Arizona, New Mexico, and Utah, *U.S. Geol. Surv. Prof. Pap.*, 521-A, 61 pp., 1969.
- Coplen, T. B., Uses of environmental isotopes, in *Regional Groundwater Quality*, edited by W. M. Alley, pp. 227–254, Van Nostrand Reinhold, New York, 1992.
- Craig, H., Isotopic variations in meteoric water, *Science*, 133, 1702–1703, 1961.
- Duffield, G. M., D. R. Buss, and D. E. Stephenson, Velocity prediction errors related to flow model calibration uncertainty, in *Calibration and Reliability in Groundwater Modeling*, edited by Karel Kover, *IAHS Publ.*, 195, 397–406, 1990.
- Duffield, G. M., J. J. Benegar, and D. S. Ward, MODFLOWT—A modular three-dimensional groundwater flow and transport model: User's manual, version 1.18, HSI GeoTrans, Inc., Sterling, Va., 1996.
- Dulaney, A. R., The geochemistry of the N-aquifer system, Navajo and Hopi Indian Reservations, northeastern Arizona, MS thesis, 209 pp., Northern Ariz. Univ., Flagstaff, 1989.
- Ericksson, E., and V. Khunakase, Chloride concentration in groundwater, recharge rate and rate of deposition of chloride in Israel Coastal Plain, *J. Hydrol.*, 7, 178–197, 1969.
- Eychaner, J. H., Geohydrology and effects of water use in the Black

- Mesa area, Navajo and Hopi Indian reservations, Arizona, *U.S. Geol. Surv. Water Supply Pap.*, 2201, 26 pp., 1983.
- Farrar, C. D., Map showing groundwater conditions in the Kaibito and Tuba City areas, Coconino and Navajo Counties, Arizona—1978, *U.S. Geol. Surv. Water Resour. Invest.*, 79-58, 1979.
- Farrar, C. D., Maps showing groundwater conditions in the Hopi area, Coconino and Navajo Counties, Arizona—1977, *U.S. Geol. Surv. Water Resour. Invest.*, 80-3, 1980.
- Fontes, J. C., Dating of groundwater, in *Guidebook on Nuclear Techniques in Hydrology, Tech. Rep. Ser.*, vol. 91, pp. 285–317, Int. At. Energy Agency, Vienna, 1983.
- Fontes, J. C., Chemical and isotopic constraints on  $^{14}\text{C}$  dating of groundwater, in *Radiocarbon After Four Decades*, edited by R. E. Taylor, A. Long, and R. S. Kra, pp. 242–261, Springer-Verlag, New York, 1992.
- Fontes, J. C., and J. M. Garnier, Determination of the initial  $^{14}\text{C}$  activity of the total dissolved carbon: A review of the existing models and a new approach, *Water Resour. Res.*, 15, 399–413, 1979.
- Freeze, R. A., and J. A. Cherry, *Groundwater*, 604 pp., Prentice Hall, New York, 1979.
- Fritz, P., E. J. Reardon, J. Barker, M. Brown, A. Cherry, W. D. Killey, and D. McNaughton, The carbon isotope geochemistry of a small groundwater system in northeastern Ontario, *Water Resour. Res.*, 14, 1059–1067, 1978.
- Garrels, R. M., and F. T. Mackenzie, Origin of the chemical composition of some springs and systems, in *Equilibrium Concepts in Natural Water Systems, Adv. in Chem. Ser.*, vol. 67, pp. 222–242, Am. Chem. Soc., Washington, D. C., 1967.
- Gee, G. W., and D. Hillel, Groundwater recharge in arid regions: Review and critique of estimate methods, *Hydrol. Processes*, 2, 255–266, 1988.
- Geyh, M. A., Carbon 14 concentration of lime in soils and aspects of the carbon 14 dating of groundwater, in *Isotope Hydrology 1970*, pp. 215–222, Int. At. Energy Agency, Vienna, 1970.
- Geyh, M. A., On the determination of the initial  $^{14}\text{C}$  content in groundwater, paper presented at Eighth International Conference on Radiocarbon Dating, R. Soc. of N. Z., Wellington, 1972.
- Gieske, A. S. M., Dynamics of groundwater recharge: A case study in semi-arid eastern Botswana, Ph.D. thesis, 289 pp., Virije Univ., Amsterdam, 1992.
- Griffith, S. R., Geochemistry and reaction path modeling of the N-aquifer system, Hopi Indian reservation, Northeastern Arizona, MS thesis, 107 pp., Univ. of Northern Ariz., Flagstaff, 1993.
- Harshbarger, J. W., C. A. Repenning, and J. H. Irwin, Stratigraphy of the uppermost Triassic and the Jurassic rocks of the Navajo country, *U.S. Geol. Surv. Prof. Pap.*, 291, 71 pp., 1957.
- Hart, R. J., and J. P. Sottolare, Progress report on the ground-water, surface-water, and quality-of-water monitoring program, Black Mesa area, northeastern Arizona—1987–88, *U.S. Geol. Surv. Open File Rep.*, 88-467, 27 pp., 1988.
- Hart, R. J., and J. P. Sottolare, Progress report on the ground-water, surface-water, and quality-of-water monitoring program, Black Mesa area, northeastern Arizona—1988–89, *U.S. Geol. Surv. Open File Rep.*, 89-383, 33 pp., 1989.
- Hendrickx, J., and G. Walker, Recharge from precipitation, in *Recharge of Phreatic Aquifers in (semi) Arid Areas*, edited by I. Simmers, pp. 19–98, A. A. Balkema, Brookfield, Vt., 1997.
- Hill, G. W., Progress report in Black Mesa monitoring program—1984, *U.S. Geol. Surv. Open File Rep.*, 85-483, 24 pp., 1985.
- Hill, G. W., and J. P. Sottolare, Progress report on the ground-water, and quality-of-water monitoring program, Black Mesa area, northeastern Arizona—1987, *U.S. Geol. Surv. Open File Rep.*, 87-458, 29 pp., 1987.
- Hill, G. W., and M. I. Whetten, Progress report on Black Mesa monitoring program—1985–86, *U.S. Geol. Surv. Open File Rep.*, 86-414, 23 pp., 1986.
- Ingerson, E., and F. J. Pearson, Estimation of age and rate of motion of groundwater by the  $^{14}\text{C}$ -method, in *Recent Researches in the Field of Hydrosphere, Atmosphere and Nuclear Geochemistry*, edited by Y. Miyake and T. Koyama, pp. 263–283, Maruzen, Tokyo, 1964.
- Kister, L. R., and J. L. Hatchett, Selected chemical analyses of the ground water, Geohydrologic data in the Navajo and Hopi Indian reservations, Arizona, New Mexico, and Utah, part 2, *Water Resour. Rep. Ariz. State Land Dep.*, 12-B, 58 pp., 1963.
- Lerner, D. N., A. S. Issar, and I. Simmers, Groundwater recharge—A guide to understanding and estimating natural recharge, *International Contribution to Hydrogeology*, vol. 8, p. 345, Velag Heinz Heise, Hannover, Germany, 1990.
- Levings, G. W., and C. D. Farrar, Maps showing groundwater conditions in the northern part of the Chinle area, Apache County, Arizona—1976, *U.S. Geol. Surv. Water Resour. Invest.*, 77-35, 1977a.
- Levings, G. W., and C. D. Farrar, Maps showing groundwater conditions in the southern part of the Black Mesa area, Arizona—1976, *U.S. Geol. Surv. Water Resour. Invest.*, 77-41, 1977b.
- Levings, G. W., and C. D. Farrar, Maps showing groundwater conditions in the Monument Valley and northern part of the Black Mesa areas, Navajo, Apache, Coconino Counties, Arizona—1976, *U.S. Geol. Surv. Water Resour. Invest.*, 77-44, 1977c.
- Levings, G. W., and C. D. Farrar, Maps showing groundwater conditions in the southern northern part of the Chinle area, Apache County, Arizona—1976, *U.S. Geol. Surv. Water Resour. Invest.*, 77-50, 1977d.
- Littin, G. R., Results of ground-water, surface-water, and water-quality monitoring, Black Mesa area, northeastern Arizona—1990–91, *U.S. Geol. Surv. Water Resour. Invest. Rep.*, 92-4045, 32 pp., 1992.
- Littin, G. R., Results of ground-water, surface-water, and water-quality monitoring, Black Mesa area, northeastern Arizona—1991–92, *U.S. Geol. Surv. Water Resour. Invest. Rep.*, 93-4111, 23 pp., 1993.
- Littin, G. R., and S. A. Monroe, Results of groundwater, surface-water and water-chemistry monitoring, Black Mesa area, northeastern Arizona—1994, *U.S. Geol. Surv. Water Resour. Invest. Rep.*, 96-4238, 25 pp., 1995.
- Lopes, T. J., and J. P. Hoffman, Geochemical analyses of groundwater ages, recharge rates, and hydraulic conductivity of the N-aquifer, Black Mesa, Arizona, *U.S. Geol. Surv. Water Resour. Invest. Rep.*, 96-4190, 1997.
- Maxey, G. B., and T. E. Eakin, Groundwater in White River valley, White Pine, Nye and Lincoln Counties, Nevada, *Nev. State Eng. Water Resour. Bull.*, 8, 59 pp., 1949.
- McDonald, M. G., and A. W. Harbaugh, A modular three-dimensional finite-difference groundwater flow model, *Techniques Water Resour. Invest. U.S. Geol. Surv.*, 06-A1, 576 pp., 1988.
- Merlivat, L., and J. Jouzel, Global climatic interpretation of the deuterium-oxygen 18 relationship for precipitation, *J. Geophys. Res.*, 84, 5029–5033, 1979.
- Mook, W. G., On the reconstruction of the initial  $^{14}\text{C}$  content of groundwater from the chemical and isotopic composition, in *Proceedings of the 8th International  $^{14}\text{C}$  Conference*, edited by T. A. Rafter and G. Taylor, pp. 342–352, R. Soc. of N. Z., Wellington, 1972.
- Mook, W. G., The dissolution-exchange model for dating groundwater with  $^{14}\text{C}$ , in *Interpretation of Environmental Isotope and Hydrochemical Data in Groundwater Hydrology*, pp. 213–225, Int. At. Energy Agency, Vienna, 1976.
- Mook, W. G., Carbon-14 in hydrogeological studies, in *Handbook of Environmental Isotopes Geochemistry*, edited by P. Fritz and J. C. Fontes, pp. 50–74, Elsevier Sci., New York, 1980.
- National Research Council (NRC), *Groundwater Models—Scientific and Regulatory Applications*, Natl. Acad. Press, Washington, D. C., 1990.
- Pearson, F. J., Jr., Use of C-13/C-12 ratios to correct radiocarbon ages of material initially diluted by limestone, paper presented at Sixth International Conference on Radiocarbon, U.S. At. Energy Comm., Pullman, Wash., 1965.
- Pearson, F. J., Jr., and B. B. Hanshaw, Sources of dissolved carbonate species in groundwater and their effects on carbon-14 dating, in *Isotope Hydrology 1970*, pp. 271–285, Int. At. Energy Agency, Vienna, 1970.
- Phillips, F. M., Environmental tracers for water movement in desert soils of the American southwest, *Soil Sci. Soc. Am. J.*, 58, 15–24, 1994.
- Phillips, F. M., M. Tansey, L. A. Peters, S. Cheng, and A. Long, An isotopic investigation of ground water in the central San Juan Basin, New Mexico: Carbon 14 dating as a basis for numerical flow modeling, *Water Resour. Res.*, 25, 2259–2273, 1989.
- Plummer, L. N., J. F. Busby, R. W. Lee, and B. B. Hanshaw, Geochemical modeling of the Madison-aquifer in parts of Montana, Wyoming and South Dakota, *Water Resour. Res.*, 26, 1981–2014, 1990.
- Plummer, L. N., E. C. Prestemon, and D. L. Parkhurst, NET-PATH—An interactive code for modeling NET geochemical reac-

- tions along a flow PATH, *U.S. Geol. Surv. Water Resour. Invest. Rep.*, 91-4078, 227 pp., 1991.
- Poeter, E. P., and M. C. Hill, Inverse models: A necessary next step in ground-water modeling, *Groundwater*, 35, 250–260, 1997.
- Portniaguine, O., and D. K. Solomon, Parameters estimation using groundwater ages and head data, Cape Cod, Massachusetts, *Water Resour. Res.*, 34, 637–645, 1998.
- Reilly, T., L. N. Plummer, P. J. Phillips, and E. Busenburg, The use of simulation and multiple environmental tracers to quantify ground-water flow in a shallow aquifer, *Water Resour. Res.*, 30, 421–433, 1994.
- Repenning, C. A., and H. G. Page, Late Cretaceous stratigraphy of the Black Mesa, Navajo and Hopi Indian reservations, Arizona, *AAPG Bull.*, 40, 255–294, 1956.
- Robertson, F. F., Radiocarbon dating of groundwater in a confined aquifer in southeast Arizona, *Radiocarbon*, 34(3), 664–676, 1992.
- Robertson, W. D., and A. C. Cherry, Tritium as an indicator of recharge and dispersion in a groundwater system in central Ontario, *Water Resour. Res.*, 25, 741–755, 1989.
- Simmers, I., Groundwater recharge principles, problems, and developments, in *Recharge of Phreatic Aquifers in (semi) Arid Areas*, edited by I. Simmers, pp. 1–18, A. A. Balkema, Brookfield, Vt., 1997.
- Solomon, D. K., and E. A. Sudicky, Tritium and helium 3 isotope ratios for direct estimation of spatial variation in groundwater recharge, *Water Resour. Res.*, 27, 2309–2319, 1991.
- Sun, N. Z., *Inverse Problems in Groundwater Modeling*, 337 pp., Kluwer Acad., Norwell, Mass., 1994.
- Sun, N. Z., and W. W. G. Yeh, Coupled inverse problems in ground-water modeling, 1, Sensitivity analysis and parameter identification, *Water Resour. Res.*, 26, 2507–2525, 1990.
- Tamers, M. A., Radiocarbon ages of groundwater in an arid zone unconfined aquifer, in *Isotope Techniques in the Hydrological Cycle*, *Geophys. Monogr. Ser.*, vol. 11, edited by G. E. Stout, pp. 143–152, AGU, Washington, D. C., 1967a.
- Tamers, M. A., Surface-water infiltration and groundwater movement in arid zones of Venezuela, in *Isotopes in Hydrology*, pp. 339–351, Int. At. Energy Agency, Vienna, 1967b.
- Tamers, M. A., Validity of radiocarbon dates on groundwater, *Surv. Geophys.*, 2, 217–239, 1975.
- Trusdell, A. H., and B. F. Jones, Wateq—A computer program for calculating chemical equilibria of natural waters, *J. Res. U.S. Geol. Surv.*, 2(2), 233–248, 1974.
- Vogel, J. C., Investigations of groundwater flow with radiocarbon, in *Isotopes in Hydrology*, pp. 355–368, Int. At. Energy Agency, Vienna, 1967.
- Vogel, J. C., Carbon-14 dating of groundwater, in *Isotope Hydrology 1970*, pp. 235–237, Int. At. Energy Agency, Vienna, 1970.
- Wallick, E. I., Isotopic and chemical considerations in radiocarbon dating of groundwater within the semiarid Tucson Basin, Arizona, in *Interpretation of Environmental Isotope and Hydrochemical Data in Groundwater Hydrology*, pp. 195–212, Int. At. Energy Agency, Vienna, 1976.
- Wickham, M., The geochemistry of surface water and groundwater interactions for selected Black Mesa drainage, Little Colorado river basin, Arizona, MS, 249 pp., Univ. of Ariz., Tucson, 1992.
- Wigley, T. M. L., Carbon dating of groundwater from closed and open systems, *Water Resour. Res.*, 11, 324–328, 1975.
- Wigley, T. M., L. N. Plummer, and F. J. Pearson, Mass transfer and carbon isotope evolution in natural water systems, *Geochim. Cosmochim. Acta*, 42, 1117–1139, 1978.
- Wood, W. W., and W. E. Sanford, Chemical and isotopic methods for quantifying ground-water recharge in a regional, semi-arid environment, *Ground Water*, 33(3), 458–468, 1995.
- Zhu, C., R. K. Waddell, I. Star, and M. Ostrander, The responses of groundwater in the Black Mesa basin, northeastern Arizona to paleoclimatic changes during late Pleistocene and Holocene, *Geology*, 26, 127–130, 1998.

---

C. Zhu, Department of Geology and Planetary Science, University of Pittsburgh, Pittsburgh, PA 15260.

(Received April 1, 1999; revised May 23, 2000; accepted May 23, 2000.)